Attempting to Reconstruct an Ancient Convergent Margin: Geospatial Analysis of the Mesoproterozoic Barby Formation in the Konkiep Group in SW Namibia

Katelyn M. Lehman, Dr. Richard Hanson, Professor Tamie Morgan

Student Research Symposium, April 2018,Texas Christian University, Fort Worth, TX

SCHOOL OF Geology, Energy & the Environment

TCU COLLEGE OF SCIENCE & ENGINEERING

ABSTRACT

The ~1.2 billion-year-old-Barby Formation located in SW Namibia has been argued to represent a continental volcanic arc. Recent research by our group (see other poster by Lehman et al.) has supported these arguments with data exhibiting steeply dipping, light-rare-earth-element enriched patterns, negative Nb/Ta anomalies, and calc-alkaline andesitic to shoshonitic compositions. The shoshonitic rocks are particularly interesting as these compositions often form in unusual arc settings (i.e., flat-slab subduction, oblique subduction, ridge subduction). Pearce et al. (2005) showed that the relative plate depth, and in turn, subduction angle and orientation can be interpreted by mapping diagnostic trace element ratios. The spatial distribution of the geochemical ratios could potentially also differentiate between shoshonitic volcanic rocks formed as a result of unusual plate geometries as opposed to a slab tear. If the map displays a tight cluster of shoshonitic composition rocks, the samples more likely formed above a slab tear, while a dispersed arrangement would be more suggestive of either a flat-slab or oblique subduction origin. ArcGis Pro was used to map and analyze XRF and ICP-MS data from 20 samples of the Barby Formation. The samples are from lava flows or sills and range from calc-alkaline to shoshonitic in composition. Both spatial tools and statistical analysis tools were used in an effort to explore potential geospatial relationships of key trace element ratios and previously established geochemical clusters. These results were then employed to attempt to recreate the subduction conditions that formed this volcanic arc.

BACKGROUND

KONKIEP TERRANE

Located in south-west Namibia, the Konkiep Terrane has played an important role in reconstructing the formation of the Namaqua-Natal Orogenic Belt (NNOB) (Figure 1). The NNOB represents the ancient southern continental margin of the Kalahari Craton (e.g., Jacobs et al., 1993, 2008; Dalziel et al., 2000; Eglington and Armstrong, 2003). During the Mesoproterozoic, the NNOB acted as a major convergent margin, which underwent arc accretion, arc/microcontinent collision, continent-continent collision and intraplate magmatism (e.g., Hanson et al., 2006; Miller, 2012; Cornell et al., 2015). This extensive orogenic belt formed during the large-scale accretionary event which ended in the formation of the supercontinent Rodinia at ~1 Ga (e.g., Hanson, 2003; Becker et al., 2006; Jacobs et al., 2008).

The Konkiep Terrane may represent the oldest relatively unmetamorphosed Mesoproterozoic crust within the NNOB (Miller, 2008). The Konkiep Terrane is composed of amphibolitic basement termed the Gorrasis group (informal term), which is unconformably overlain by the relatively undeformed Konkiep Group comprises six volcanic formations with associated intrusive units, and two sedimentary formations (Miller, 2008) (Figure 2). Table 1, modified from Miller (2008), summarizes the lithology of the sedimentary and volcanic rocks. The Konkiep Group has undergone very low-grade metamorphism (zeolite and prehnite-pumpellyite facies) with depositional features, volcanic textures, and some primary mineralogy preserved (Miller, 2012). This lack of deformation, combined with the early time of accretion of at least part of the Konkiep Terrane (>1.33 Ga) and active magmatism until 1.1 Ga, provides a window into the tectonic and magmatic changes that occurred in this part of the NNOB (Panzik et al., 2015; Cornell et al., 2015).

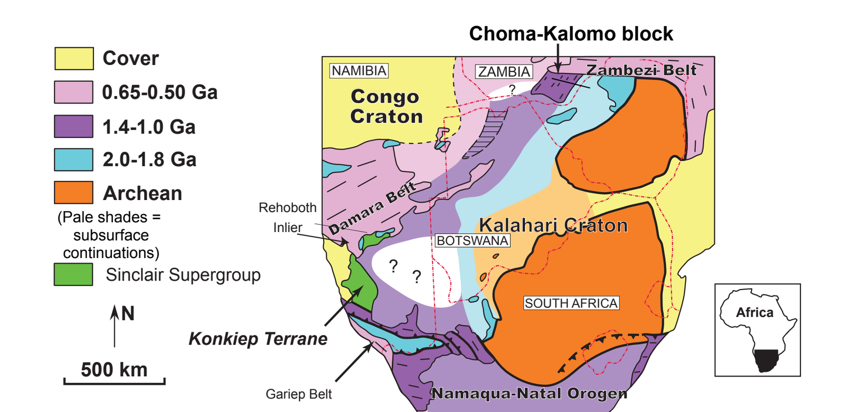

Figure 1: Simplified geologic map of southern Africa. Colors represent predominant rock ages in the region. Note the Sinclair Supergroup and Konkiep Terrane is highlighted in green and is considered to be a part of the NNOB. Map modified from Hanson (2003) and Panzik et al. (2006).

Figure 3: Photo of the Baby Formation taken by Virginia Andrews. Photo location noted in Figure 2 looking North. Sill Packages makeup central region of photo.

Konkiep Group			
Formation	**Lithology**	**Maximum Thickness (m)**	**Age (Ma)**
Aubures (Miller, 2008)	Dark rust red shales, rust red lithic to arkosic sandstones, polymictic conglomerates, Basal polymictic conglomerate	2590	1108 ± 9 (Kasbohm et al, 2016)
Guperas	Quartz porphyry lava, block and ash flows	1000	
	Basic lava		
	polymictic conglomerate, lithic sandstone		
	Green shale		
	Brown to grey polymictic conglomerate, purple-red lithic sandstone, quartzite	3700	
Barby (von Brunn, 1969; Watters, 1974)	Aruab Mountain: Cross-bedded orthoquartzite, feldspathic quartzite	400	1214 ± 5(Cornell et al., 2016) to 1217 ± 2 (Cornell et al., unpublished)
	volcaniclastic and lithic sandstone, conglomerate		
	Pyroxene trachyandesite lavas and tuffs;	400	
	Pyroxene trachybasalt lavas;	5800	
	Basaltic andesite lavas;	3150	
	Large-feldspar trachyandesite lavas;	1400	
	Small-feldspar trachyandesite lavas;	1300	
	Latite;	2000	
	Volcaniclastic sandstone	1550	
	Rhyolitic pyroclastic rocks	80	
Haiber Flats (Hoal, 1990)	Porphyritic rhyolite and ignimbrite, minor rhyodacite, interbedded volcaniclastic sandstone	120	
	Phyric and amygdaloidal basaltic andesite and andesite, occasionally pyroclastic, tuff, rhyolite and volcaniclastic sediment		
Kunjas	Lithic sandstone, polymict conglomerate;		1304 ± 1 (Cornell et al., unpublished data)- youngest detrital zircon grains
	Shale, minor rhyolitic and mafic volcanic layers, iron formation;		
	Basal conglomerate overlain by lithic sandstone (Watters, 1974)	300	
	Shale	1200	
	Pebbly lithic and arkosic sandstone, minor polymict conglomerate		
	siltstone, minor sandy limestone, red chert	100	
	Basal polymict conglomerate overlain by lithic sandstone, subarkose (Hoal, 1990)	800	
Welverdiend	Tholeiitic basalts, agglomerates, rhyolites and associated tuff, volcaniclastic and clastic sedimentary rocks		1327 ± 10 (Cornell et al., 2015)
Nagatis (von Brunn, 1967)	Pyroclastic quartz porphyry, ignimbrite layers at base, interbedded basic lava in middle of unit	1000	1363 ± 11 (Cornell et al., 2016)
	Polymict conglomerate, volcaniclastic grit and lithic sandstone, arkose, shale		
	Mafic lava, altered mafic lava		
	Block and Ash	1000	
	Felsic lavas, ignimbrite		
Kairab	Porphyritic mafic and felsic metavolcanic rocks	4000	1369 ± 10 (Cornell et al., 2016)
(Hoal, 1990)	minor volcaniclastic metasediment		
Gorrasis (Miller, 2008)	Basement		1372 ± 12 (Cornell et al., 2016)

Table 1 (to the right: Lithological descriptions of the volcanic and sedimentary rock formations that make up the Konkiep Group. Ages and maximum thickness of each unit are noted. Table modified from Miller (2008). Colors correspond to Figure 2.

BARBY FORMATION

The ~1.2 Ga Barby Formation has been the most researched formation of the Konkiep Group and is, arguably, the most complex volcanic unit within the group. The calc-alkaline to shoshonitic formation is preserved in extensional basins and is estimated to be <8500 m thick (Miller, 2008). Syndepositional faults, which indicate a lateral movement component, cut the formation (Watters, 1974; Brown and Wilson, 1986). Large feldspar-phyric intermediate lavas are characteristic of the Barby Formation and have been termed trachyandesites by previous researchers. Based on the high K_2O, high Zr, lack of iron enrichment, depletion in TiO_2 and Nb, and enrichment in light rare earth elements (LREE), the Barby Formation has been argued to consist of calc-alkaline to shoshonitic volcanic rocks that formed in a continental arc setting (Watters, 1974, 1977; Hoal, 1990, 1993; Brown and Wilson, 1996; Miller, 2008, 2012) (Figure 4). The presence of shoshonitic compositions could suggest that the Barby Formation formed in unusual arc settings, possibly related to oblique or flat-slab subduction (e.g., Becker et al., 2006; Kay and Mpdozis, 2002).

Previous studies heavily relied on mobile element data to makes these petrotectonic arguments (Watters, 1974; Brown and Wilson, 1986). The mobile element concentrations are likely to have been altered by secondary processes, making these data unreliable for constraining petrologic processes. This study utilizes major element and trace element data, particularly focusing on immobile element ratios from 25 samples collected in the 2016 field season.These samples were collected from the three main facies: (1) Hawaiian, Strombolian, and phreatomagmatic deposits; (2) lava flows; and (3) sill packages (Figure 3) containing two to six lithologically distinct sills intruded into lacustrine deposits (Andrews et al., 2016, 2017; Lehman et al., 2016). Sample locations are shown in Figure 2.

Problem

Can we use geospatial analysis to reconstruct ancient volcanic arcs?

Subduction Zone Geochemical Trends

Arc Volcanism

- As subducting slabs dehydrate, fluid-mobile elements, the Large Ion Lithophile elements (LIL), metasomatize mantle wedge, which is then partially melted. High water content is associated with high oxygen fugacity which can be quantified in-part through the V/Ti ratio (e.g., Best, 2003; Mallmann and O'neill, 2009).
- The dehydrated fluids or hydrous melts can metasomatize the overlying arc lithosphere, which can fractionate Nb/Ta, Zr/Sm, and Th/Yb (e.g., Pearce et al., 1990).
- The deeper the slab subducts the less fluids available from hydrous mineral breakdown which causes a decrease in LIL (e.g., Best, 2003).
- Increasing K-content of arc magmas is associated with LREE enrichment, which can be quantified via La/Yb ratio. This pattern is argued to result of fractionation involving plagioclase, clinopyroxene, olivine, and Fe-Ti oxides (e.g., Best, 2003). Extreme La/Yb values are associated with garnet in the magma source.
- Continental arcs are associated with thicker crust (high La/Yb), and depleted source (lower concentrations of High Field Strength Elements (HFSE), and incompatible elements) due to multiple stages of melting and melt extraction.
- Continental arcs characteristically produce andesite
- Melting-Assimilation-Storage and Homogenization (MASH) zone often forms in the lower crust in continental arcs

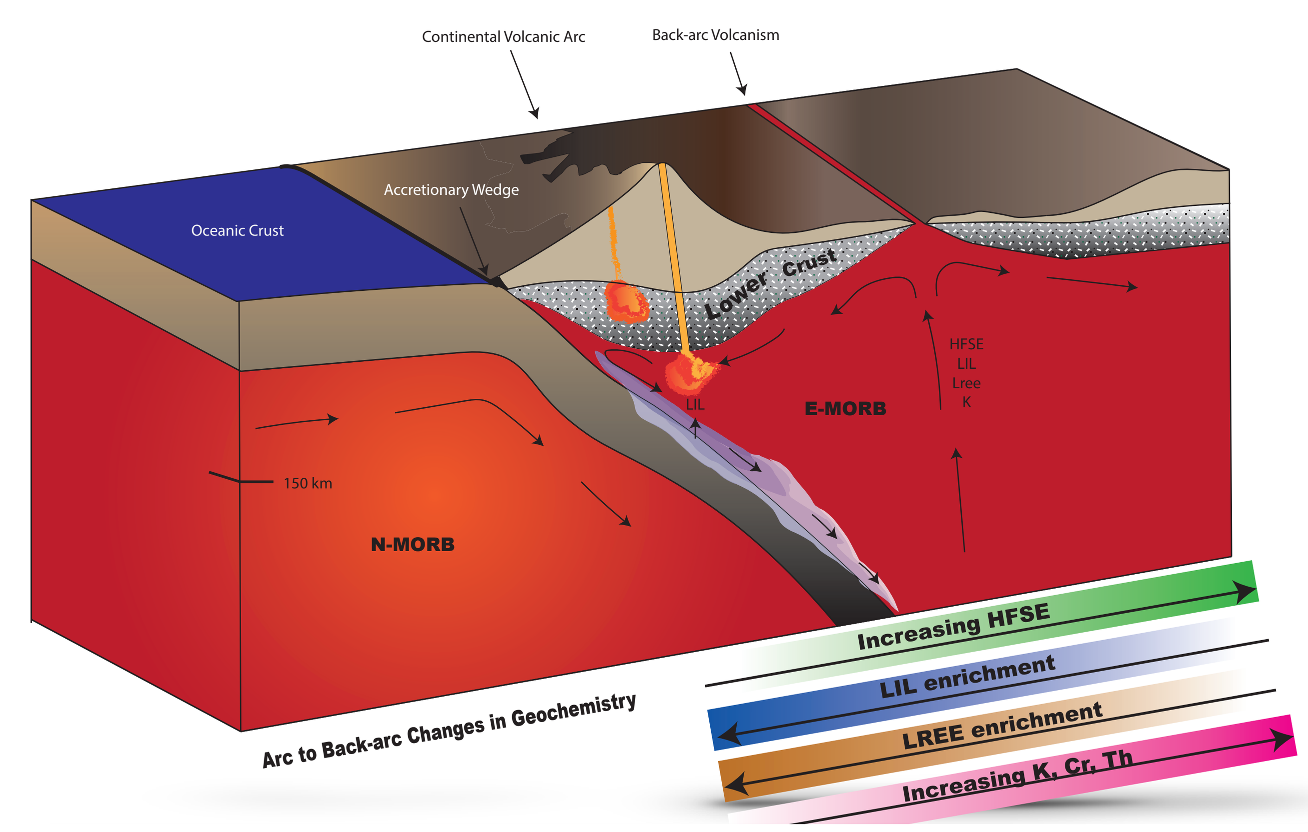

Figure 4: Schematic of the relationship between arc and back-arc volcanism in normal continental arcs (not to scale). To identify if the there is an arc-back-arc relationship these changes in geochemistry should be observable. The back-arc shows less of a subduction influence (lower oxygen fugacity, less LIL enrichment, less LREE enrichment, and comes from a less depleted source (i.e. high HFSE and K) (e.g., Sanders and Tarney, 1984; Kay & Gordillio, 1994, Woodhead et al., 1993; Best, 2003; White, 2013).

Back-arc Volcanism

- Can form due to extensional tectonics from slab drag, slab-roll back, slab break off, etc.
- Back-arc volcanism forms, in part, as a result of decompression melting from divergent forces. Back-arc magmas range from N-MORB to calcalkaline compositions, depending on the length of time the subduction zone has been establish (longer time or shallower slab appears more arc-like)
- More mantle input leads to higher HFSE, Cr, and Th.
- Thinner crust leads to lower La/Yb (lower LREE enrichment).

Other Factors

- Incorporation of subducted eroded material
- Flat-slab subduction can later cause wet-spot melting as the slab steepens
  - Produces extremely hydrous melts
  - Producing greater LIL enrichment
- Flat-slab and oblique subduction can lead to thicker crust (producing higher La/Yb ratios if garnet forms), a greater amount of subduction erosion)
- Oblique subduction will produce highly variable compositions with MORB or island arc magma compositions produce

METHODOLOGY

Samples were collected from Namibia during the Summer 2016. The samples were analyzed using ICP-MS and XRF at Washington State University. This geochemical data was analyzed using a three stage process.

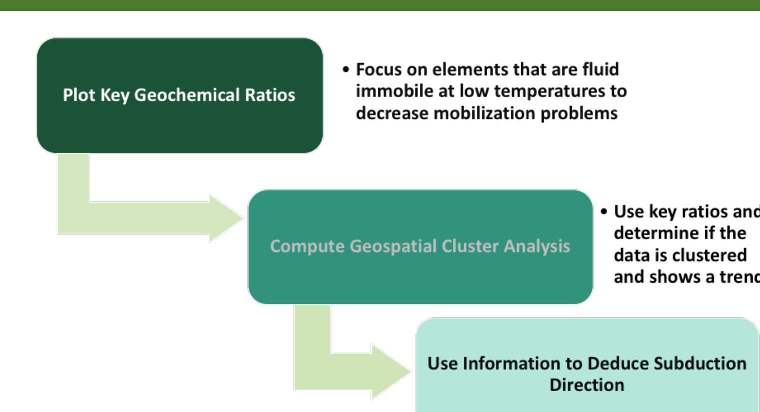

References

Becker, T., Schreiber, U., Kampunzu, A.B., and Armstrong, R., 2006, Mesoproterozoic rocks of Namibia and their plate tectonic setting: Journal of African Earth Sciences, v. 46, p. 112–140. Best, M.G., 2013, Igneous and metamorphic petrology: John Wiley & Sons. Brown, G.J., and Wilson, A.H., 1986, The petrology and geochemistry of the Barby Formation, Sinclair Sequence: Communications of the Geological Survey of South West Africa/Namibia, v. 2, p. 93–108. Cornell, D.H., Mapani, B., and Malobela, T., 2016, Precise zircon dating reveals the threefold evolution of the Sinclair Supergroup of Namibia, *in* South Africa. Cornell, D.H., van Schijndel, V., Simonsen, S.L., and Frei, D., 2015, Geochronology of Mesoproterozoic hybrid intrusions in the Konkiep Terrane, Namibia, from passive to active continental margin in the Namaqua-Natal Wilson Cycle: Precambrian Research, v. 265, p. 166–188. Dalziel, I.W., Mosher, S., and Gahagan, L.M., 2000, Laurentia-Kalahari collision and the assembly of Rodinia: The Journal of Geology, v. 108, p. 499–513. Eglington, B.M., and Armstrong, R.A., 2003, Geochronological and isotopic constraints on the Mesoproterozoic Namaqua–Natal Belt: evidence from deep borehole intersections in South Africa: Precambrian Research, v. 125, p. 179–189. Foley, S., Tiepolo, M., and Vannucci, R., 2002, Growth of early continental crust controlled by melting of amphibolite in subduction zones: Nature, v. 417, p. 837. Foley, S., Venturelli, G., Green, D.H., and Toscani, L., 1987, The ultrapotassic rocks: characteristics, classification, and constraints for petrogenetic models: Earth-Science Reviews, v. 24, p. 81–134. Green, T.H., 1995, Significance of Nb/Ta as an indicator of geochemical processes in the crust-mantle system: Chemical Geology, v. 120, p. 347–359. Hanson, R.E., 2003, Proterozoic geochronology and tectonic evolution of southern Africa: Geological Society, London, Special Publications, v. 206, p. 427–463. Hanson, R.E., Harmer, R.E., Blenkinsop, T.G., Bullen, D.S., Dalziel, I.W.D., Gose, W.A., Hall, R.P., Kampunzu, A.B., Key, R.M., and Mukwakwami, J., 2006, Mesoproterozoic intraplate magmatism in the Kalahari Craton: a review: Journal of African Earth Sciences, v. 46, p. 141–167. Hari, K.R., Rao, N.C., Swarnkar, V., and Hou, G., 2014, Alkali feldspar syenites with shoshonitic affinities from Chhotaudepur area: implication for mantle metasomatism in the Deccan large igneous province: Geoscience Frontiers, v. 5, p. 261–276. Hoal, B.G., 1990, The geology and geochemistry of the Proterozoic Awasib Mountain terrain, southern Namibia: Ministry of Mines and Energy Geological Survey of Namibia, v. 11. Hoal, B.G., 1993, The Proterozoic Sinclair Sequence in southern Namibia: intracratonic rift or active continental margin setting? Precambrian Research, v. 63, p. 143–162. Huang, J., Xiao, Y., Gao, Y., Hou, Z., and Wu, W., 2012, Nb–Ta fractionation induced by fluid−rock interaction in subduction−zones: constraints from UHP eclogite−and vein−hosted rutile from the Dabie orogen, Central−Eastern China: Journal of Metamorphic Geology, v. 30, p. 821–842. Jacobs, J., Pisarevsky, S., Thomas, R.J., and Becker, T., 2008, The Kalahari Craton during the assembly and dispersal of Rodinia: Precambrian Research, v. 160, p. 142–158.Jacobs, J., Thomas, R.J., and Weber, K., 1993, Accretion and indentation tectonics at the southern edge of the Kaapvaal craton during the Kibaran (Grenville) orogeny: Geology, v. 21, p. 203–206. Kasbohm, J., Evans, D.A., Panzik, J.E., Hofmann, M., and Linnemann, U., 2015, Palaeomagnetic and geochronological data from Late Mesoproterozoic redbed sedimentary rocks on the western margin of Kalahari craton: Geological Society, London, Special Publications, v. 424, p. SP424. 4. Kay, S.M., and Gordillo, C.E., 1994, Pocho volcanic rocks and the melting of depleted continental lithosphere above a shallowly dipping subduction zone in the Central Andes: Contributions to Mineralogy and Petrology, v. 117, p. 25–44. Kay, S.M., and Mpodozis, C., 2002a, Magmatism as a probe to the Neogene shallowing of the Nazca plate beneath the modern Chilean flat-slab: Journal of South American Earth Sciences, v. 15, p. 39–57. Kay, S.M., and Mpodozis, C., 2002b, Magmatism as a probe to the Neogene shallowing of the Nazca plate beneath the modern Chilean flat-slab: Journal of South American Earth Sciences, v. 15, p. 39–57. Lehman, Katelyn, Andrews, V.P., Hanson, R., Baylor, D., and Williams, J., 2015, A Paleogeographic Control on the Formation of Thick, Downward-growing Sill Packages Emplaced into Wet Sediments within a Mesoproterozoic Volcanic Arc in South-Central Namibia.Miller, R.M., 2012, Review of Mesoproterozoic magmatism, sedimentation and terrane amalgamation in southwestern Africa: South African Journal of Geology, v. 115, p. 417–448. Miller, R.M., 2008, The geology of Namibia: 3 volumes, Geological Survey of Namibia, p. 1564. Müller, D., 2002, Gold-copper mineralization in alkaline rocks: Mineralium Deposita, v. 37, p. 1–3. Nakamura, N., 1974, Determination of REE, Ba, Fe, Mg, Na and K in carbonaceous and ordinary chondrites: Geochimica et Cosmochimica Acta, v. 38, p. 757–775. Nardi, L.V.S., Formoso, M.L.L., Müller, I.F., Fontana, E., Jarvis, K., and Lamarão, C., 2013, Zircon/rock partition coefficients of REEs, Y, Th, U, Nb, and Ta in granitic rocks: uses for provenance and mineral exploration purposes: Chemical Geology, v. 335, p. 1–7. P. Andrews, V., Hanson, R., Marie Lehman, K., J. Baylor, D., and Williams, J., 2017, Volcanic and Hypabyssal Lithofacies in a Meszoproterozoic Volcanic Arc Sequence, Barby Formation, Southwest Namibia., doi: 10.1130/abs/2017SC-289494.Panzik, J.E., Evans, D.A.D., Kasbohm, J.J., Hanson, R., Gose, W., and Desormeau, J., 2015, Using palaeomagnetism to determine late Mesoproterozoic palaeogeographic history and tectonic relations of the Sinclair terrane, Namaqua orogen, Namibia: Geological Society, London, Special Publications, v. 424, p. SP424. 10.Pearce, J.A., 1982, Trace element characteristics of lavas from destructive plate boundaries: Orogenic andesites and related rocks, p. 528–548.Pearce, J.A., and Norry, M.J., 1979, Petrogenetic implications of Ti, Zr, Y, and Nb variations in volcanic rocks: Contributions to mineralogy and petrology, v. 69, p. 33–47.Pearce, J.A., and Stern, R.J., 2006a, Origin of back−arc basin magmas: Trace element and isotope perspectives: Back-Arc Spreading Systems: Geological, Biological, Chemical, and Physical Interactions, p. 63–86.Pearce, J.A., and Stern, R.J., 2006b, Origin of back−arc basin magmas: Trace element and isotope perspectives: Back-Arc Spreading Systems: Geological, Biological, Chemical, and Physical Interactions, p. 63–86.Saunders, A.D., and Tarney, J., 1984, Geochemical characteristics of basaltic volcanism within back-arc basins: Geological Society, London, Special Publications, v. 16, p. 59–76.Sommer, C.A., Lima, E.F., Nardi, L.V., Liz, J.D., and Waichel, B.L., 2006, The evolution of Neoproterozoic magmatism in Southernmost Brazil: shoshonitic, high-K tholeiitic and silica-saturated, sodic alkaline volcanism in post-collisional basins: Anais da Academia Brasileira de Ciências, v. 78, p. 573–589.Stolz, A.J., Jochum, K.P., Spettel, B., and Hofmann, A.W., 1996, Fluid-and melt-related enrichment in the subarc mantle: Evidence from Nb/Ta variations in island-arc basalts: Geology, v. 24, p. 587–590.Sun, S.-S., and McDonough, W., 1989, Chemical and isotopic systematics of oceanic basalts: implications for mantle composition and processes: Geological Society, London, Special Publications, v. 42, p. 313–345.Turner, S., Arnaud, N., LIU, J., Rogers, N., Hawkesworth, C., Harris, N., Kelley, S., Van Calsteren, P., and Deng, W., 1996, Post-collision, shoshonitic volcanism on the Tibetan Plateau: implications for convective thinning of the lithosphere and the source of ocean island basalts: Journal of petrology, v. 37, p. 45–71.Von Brunn, V., 1967, Acid and basic igneous rock associations west of Helmeringhausen, South West Africa:Von Brunn, V., 1969, Igneous Rocks of the Nagatis and Sinclair Formations North-east of Lüdertiz [sic] South West Africa: University of Cape Town, Precambrian Research Unit.Watters, B.R., 1974, Stratigraphy, igneous petrology and evolution of the Sinclair Group in southern South West Africa: University of Cape Town.Watters, B.R., 1977, The Sinclair Group: definition and regional correlation: South African Journal of Geology, v. 80, p. 9–16.White, W.M., 2013, Geochemistry: Wiley Online Library.Woodhead, J., Eggins, S., and Gamble, J., 1993a, High field strength and transition element systematics in island arc and back-arc basin basalts: evidence for multi-phase melt extraction and a depleted mantle wedge: Earth and Planetary Science Letters, v. 114, p. 491–504.Woodhead, J., Eggins, S., and Gamble, J., 1993b, High field strength and transition element systematics in island arc and back-arc basin basalts: evidence for multi-phase melt extraction and a depleted mantle wedge: Earth and Planetary Science Letters, v. 114, p. 491–504.Zhang, H.-F., Sun, M., Zhou, X.-H., Fan, W.-M., Zhai, M.-G., and Yin, J.-F., 2002, Mesozoic lithosphere destruction beneath the North China Craton: evidence from major-, trace-element and Sr–Nd–Pb isotope studies of Fangcheng basalts: Contributions to Mineralogy and Petrology, v. 144, p. 241–254.

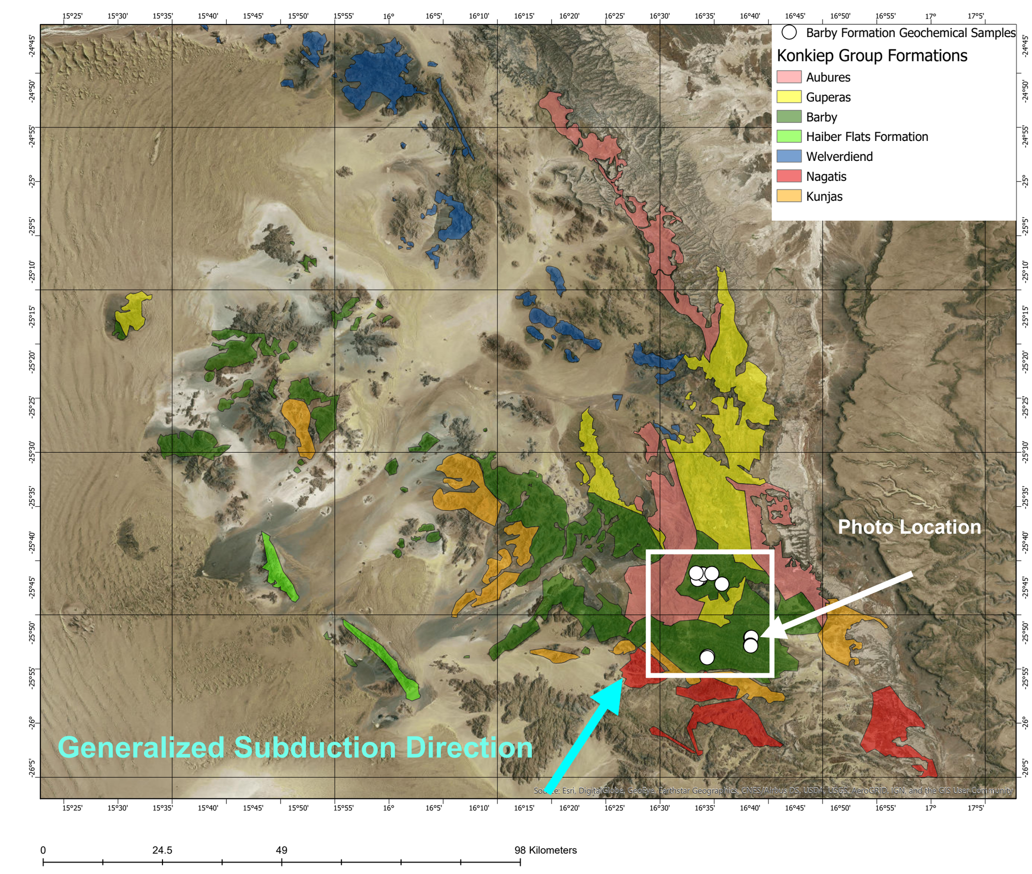

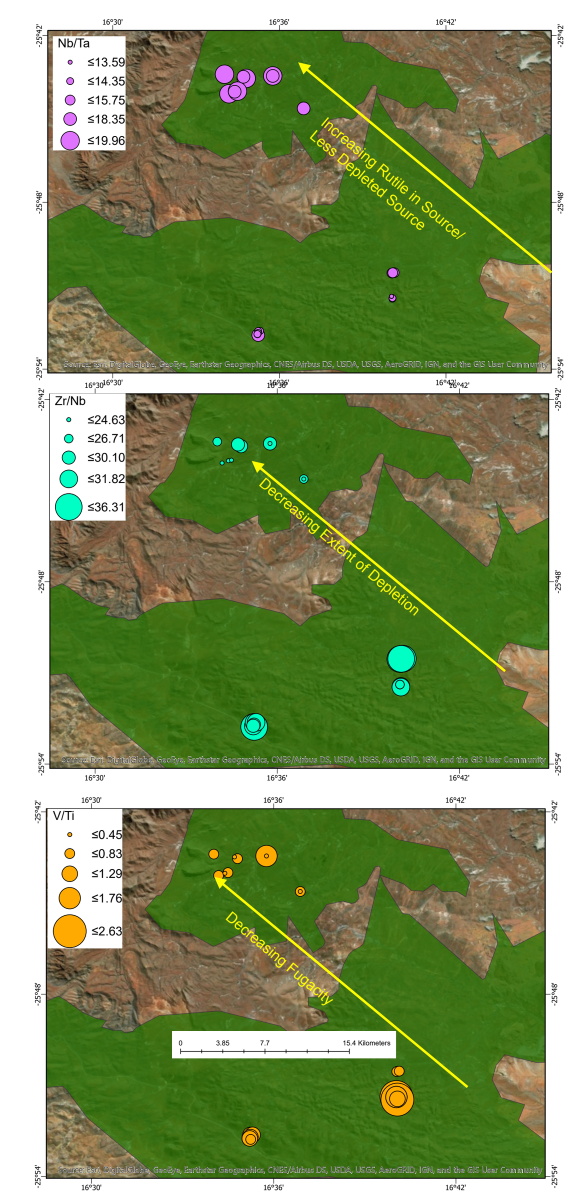

Figure 5: N-S trending element ratio differences. A. Nb/Ta is an effective indicator of source enrichment and mantle source metasomatism (Pearce & Stern, 2006). B. Zr/Nb decreases in the transition from arc to back-arc and also decreases due to less depletion in the source (e.g., Weyer et al., 2003; Pearce & Stern, 2006) C. V/Ti are controlled, in part, by oxygen fugacity (Mallmann and O'neill, 2009). V/Ti decreases from arc to back-arc (Figure 4).

Figure 2: Simplified Map of Konkiep Terrane using Miller (2008) map and ArcGIS DigitalGlobe satellite data as an underlay. Unit colors are shown in both the key and Table 1. See Figure 1 for location reference for the Konkiep Terrane. Field Site is outlined in black. Arrow points to possible generalized subduction direction assuming the northern samples are in the back-arc of the southern samples.

No Geospatial Relationship

- High La/Yb = residual garnet in source
- High Ta/Yb = continental crust assimilation/ incorporation

Grouping Analysis

- Northern Group
  - Typically plots as island arc andesites (see other Lehman et al., 2018 poster)
- Southern Group
  - Typically plots a continental arc (see other Lehman et al., 2018 poster)
  - More depleted source (lower Sm/Hf, Ti/Zr, Nb/Ta, higher Zr/Y)
  - Higher oxygen fugacity (higher V/Ti, lower Ti/Zr)
  - More lithosphere input (higher Ti/(Hf*Sm)

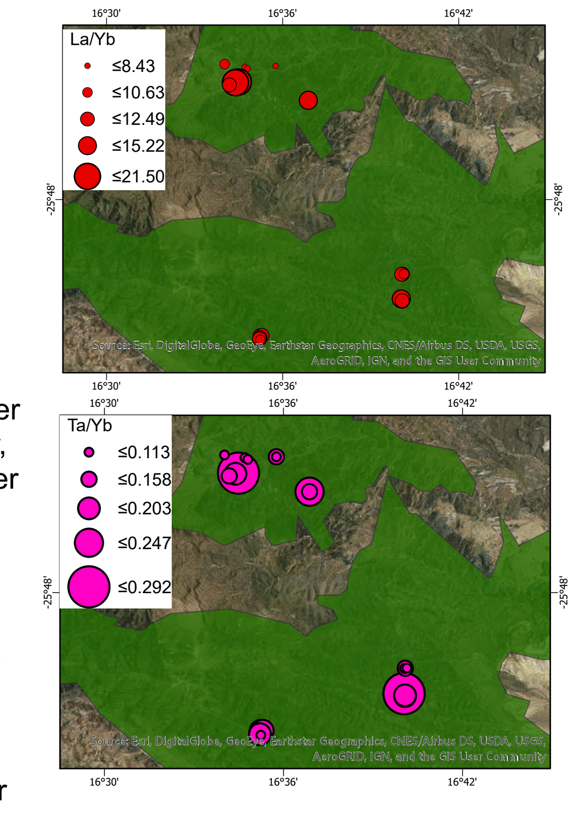

Figure 6: (left) (A) La/Yb ratio geospatial relationships. Note the dispersed nature indicating differences in the amount of residual garnet in the source (White, 2013). (B) Ta/Yb ratios are used to determine mantle enrichment and/or oceanic or continental arc setting (Pearce & Norry, 1979).

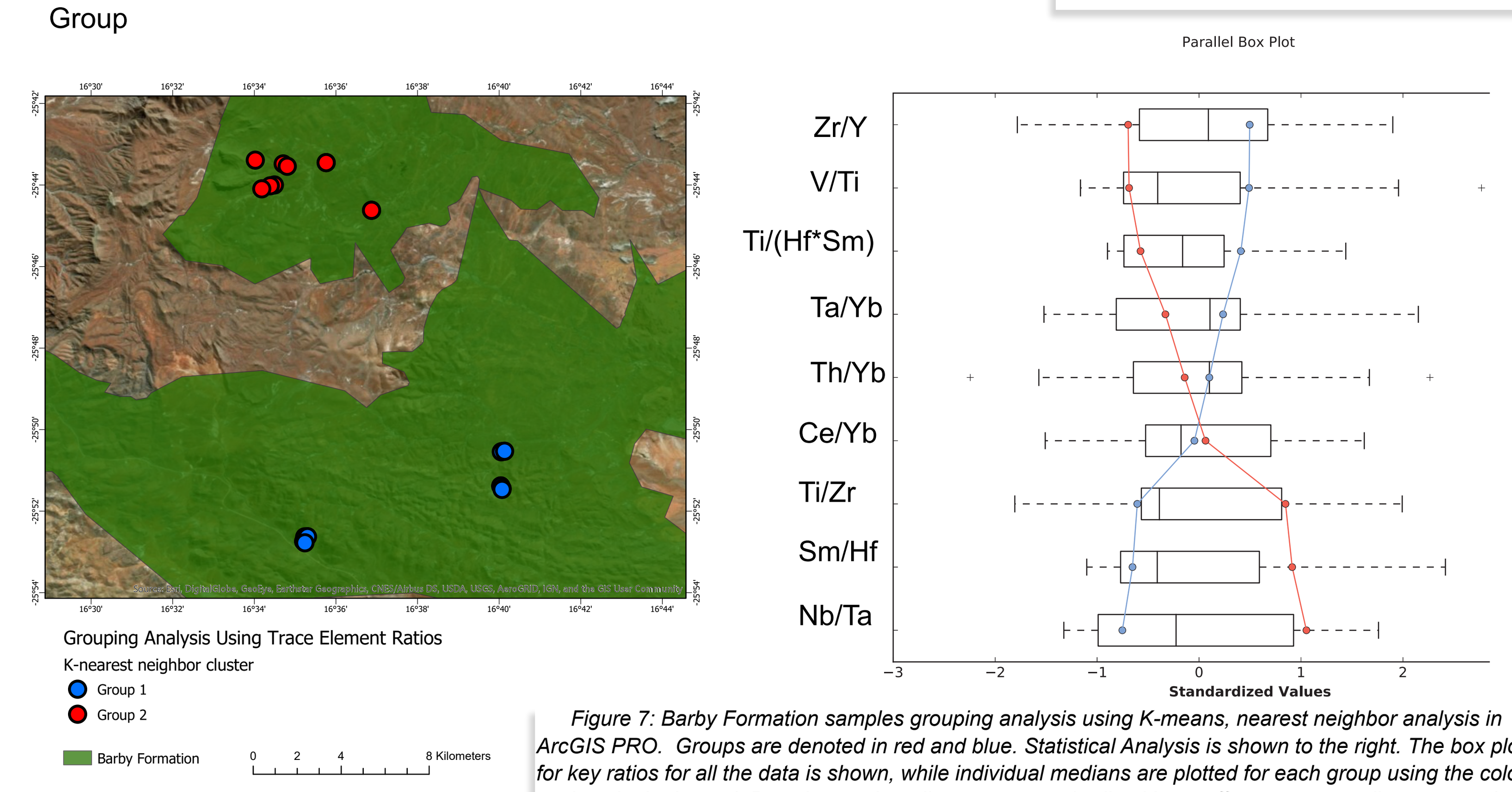

Figure 7: Barby Formation samples grouping analysis using K-means, nearest neighbor analysis in ArcGIS PRO. Groups are denoted in red and blue. Statistical Analysis is shown to the right. The box plots for key ratios for all the data is shown, while individual medians are plotted for each group using the colors given in the legend. Box plots and medians were standardized in an effort to more easily compare the different ratios. Note how the Northern and Southern samples have dramatically different medians depending on the trace element ratio.

Conclusions

Geospatial analysis is a powerful tool in reconstructing ancient volcanic arcs. The analysis elucidates spatial patterns within the Barby Formation. These patterns illustrate two environments which produced the northern and southern samples. Although all samples formed in an arc setting, the northern samples formed from a more enriched source that has lower oxygen fugacity, suggestive of formation in a back-arc or when the arc was more immature. If the northern samples do indeed represent the back-arc of the southern samples, the trench would be located in the south. The ratios that do not follow a N-S trend suggest possible incorporation of subjected eroded or delaminated lithosphere in the mantle source.